Thin Solid Films 517 (2009) 2048–2054

Contents lists available at ScienceDirect

Thin Solid Films

journal homepage: www.elsevier.com/locate/tsf

Titanium–silicon oxide film structures for polarization-modulated infrared reflection absorption spectroscopy

Iain E. Dunlop [a,f,1], Stefan Zorn [d,1], Gunther Richter [b], Vesna Srot [c], Marion Kelsch [c], Peter A. van Aken [c], Maximilian Skoda [d,e], Alexander Gerlach [d], Joachim P. Spatz [a,f], Frank Schreiber [d,*]

[a] Department of New Materials and Biosystems, Max Planck Institute for Metals Research, Heisenbergstrasse 3, 70569 Stuttgart, Germany
[b] Central Scientific Facility Thin Film Laboratory, Max Planck Institute for Metals Research, Heisenbergstrasse 3, 70569 Stuttgart, Germany
[c] Stuttgart Center for Electron Microscopy, Max Planck Institute for Metals Research, Heisenbergstrasse 3, 70569 Stuttgart, Germany
[d] Institute for Applied Physics, Eberhard-Karls University of Tübingen, Auf der Morgenstelle 10, 72076 Tübingen, Germany
[e] Physical and Theoretical Chemistry Laboratory, Oxford University, Oxford OX1 3QZ, United Kingdom
[f] Department of Biophysical Chemistry, University of Heidelberg, INF 253, 69120 Heidelberg, Germany

ARTICLE INFO

Article history:
Received 19 February 2008
Received in revised form 17 October 2008
Accepted 23 October 2008
Available online 31 October 2008

Keywords:
Biotin–streptavidin binding
Electron energy loss spectroscopy (EELS)
Fourier transform infrared spectroscopy
Poly(ethylene glycol)
Protein resistant surfaces
Silicon oxide
Titanium
Transmission electron microscopy (TEM)
X-ray photoelectron spectroscopy (XPS)
X-ray reflectometry

ABSTRACT

We present a titanium–silicon oxide film structure that permits polarization modulated infrared reflection absorption spectroscopy on silicon oxide surfaces. The structure consists of a ~6 nm sputtered silicon oxide film on a ~200 nm sputtered titanium film. Characterization using conventional and scanning transmission electron microscopy, electron energy loss spectroscopy, X-ray photoelectron spectroscopy and X-ray reflectometry is presented. We demonstrate the use of this structure to investigate a selectively protein-resistant self-assembled monolayer (SAM) consisting of silane-anchored, biotin-terminated poly(ethylene glycol) (PEG). PEG-associated IR bands were observed. Measurements of protein-characteristic band intensities showed that this SAM adsorbed streptavidin whereas it repelled bovine serum albumin, as had been expected from its structure.

1. Introduction

Infrared reflection absorption spectroscopy (IRRAS), also known as reflection absorption infrared spectroscopy (RAIRS) is a popular method of characterizing self-assembled monolayers and similar systems, enabling surface coverage, the chemical nature of the monolayer, and often additional information such as chain tilt angles to be determined (see for example Buffeteau et al. [1], Zamlynny et al. [2,3], Greenler [4], Käfer et al. [5], Hoffmann et al. [6], Skoda et al. [7], Zawisza et al. [8]).

Polarization-modulated infrared reflection absorption spectroscopy (PM-IRRAS, first introduced by Dowrey and Marcott [9]) is a powerful method of achieving high signal to noise ratios when measuring IRRAS spectra of thin film samples on conducting substrates, since the PM-IRRAS signal contains the effects of adsorbing species that lie close to the substrate surface, but is not affected by adsorbing species elsewhere in the optical path. When electromagnetic radiation is reflected by a conducting surface at grazing incidence, the amplitude of the s- and p-polarized electric field vectors near the surface differs greatly, with the s-polarized electric field amplitude being approximately zero within a distance of the order of magnitude of one wavelength of the surface, whereas the p-polarized electric field amplitude is much higher in this region [4,10]. If a conducting substrate bears a film whose thickness is much less than the wavelength of the infrared light, the spectrum of the film can thus be obtained by effectively subtracting a measured s-polarized IRRAS spectrum from its p-polarized counterpart. PM-IRRAS instruments achieve this by rapidly modulating the polarization and using a lock-in amplifier to extract the signal [9]; IRRAS spectra with a very high signal to noise ratio can thus be obtained.

Although PM-IRRAS provides high-quality data, it only works on highly conducting, usually metal, surfaces thus excluding many substrate surfaces of scientific interest, notably the silicon oxide surfaces that are commonly used in a wide variety of surface chemistry studies. The reaction of silicon oxide surfaces with silane molecules is one of the most common methods for preparing covalently grafted thin layers of organic molecules on hard substrates. The use of silicon oxide surfaces has several advantages for particular applications, such as the relative cheapness of glass (silicon oxide) substrates, the suitability of glass

* Corresponding author.
E-mail address: frank.schreiber@uni-tuebingen.de (F. Schreiber).
[1] These authors contributed equally to this work.

0040-6090/$ – see front matter © 2008 Elsevier B.V. All rights reserved.
doi:10.1016/j.tsf.2008.10.058

coverslips for transmitted light microscopic measurements in studies of the interactions between organically functionalized surfaces and biological cells [11], and the suitability of silicon and silica substrates for neutron reflectivity measurements [12,13].

In order to perform PM-IRRAS on silicon oxide, a thin film of silicon oxide should be deposited on a conducting substrate. Provided the silicon oxide thickness is much less than the infrared wavelengths in use (about 2.5–25 μm), the spectrum of any organic film deposited on top of it will be measurable.

Gold is often used as a conducting substrate in PM-IRRAS experiments, however, thin silicon oxide films directly deposited on gold are often unstable. Despite this difficulty, thin silicon oxide films on gold substrates have been produced by sol–gel methods [14,15], and using plasma-enhanced chemical vapour deposition [8,16]. Additionally, stable thin silicon oxide films on gold have been produced using an electron beam evaporation method, with an intervening thin layer of titanium between the gold and the silicon oxide [17].

Zawisza et al. [8] recently performed PM-IRRAS studies of Langmuir–Blodgett lipid layers on a substrate consisting of a thin (7–40 nm) silicon oxide film deposited by chemical vapour deposition onto a gold substrate. In this paper, we present an alternative approach to performing PM-IRRAS on a silicon oxide surface, in which we exploit the intrinsic stability of the silicon oxide–titanium interface by sputtering a thin silicon oxide layer directly onto a thick titanium layer which acts as the conducting substrate. We have thoroughly characterized this silicon oxide thin film using conventional and scanning transmission electron microscopy, X-ray reflectometry and X-ray photoelectron spectroscopy, showing it to be a rather uniform film of thickness of order 5 nm, which closely follows the contours of the titanium surface.

As a proof-of-principle for this method and illustration of its possible uses, we present a PM-IRRAS investigation of a polymer self-assembled monolayer [18–20] that is designed to selectively adsorb and repel different proteins. Both the polymer layer itself, and its protein adsorption properties are studied spectroscopically. This functionalized polymer is bound to the silicon oxide surface via a trimethoxysilane group, confirming that the sputtered silicon oxide film is chemically accessible to silane reagents, thus confirming its suitability for many possible surface chemistry studies.

Although the present measurements have been carried out in air, our substrate could also readily be used to perform PM-IRRAS under water (see for example Skoda et al. [7]).

2. Materials and methods

2.1. Thin film deposition

Novel substrates consisted of a supporting crystalline silicon wafer (<100> surface, native oxide layer not removed) onto which titanium followed by silicon oxide layers were direct current sputtered (Ti target, 99.995% pure, FHR Anlagenbau GmbH, Germany, magnetron power 100 W, argon pressure 3×10^{-3} mbar and SiO_2 target, 99.995% pure, Kurt J. Lesker Company, U.S.A., magnetron power 100 W, argon pressure 6×10^{-3} mbar). The vacuum system was homebuilt. The vacuum was not broken between the sputtering of the two layers. Layer thicknesses were nominally 200 nm for the titanium layer and 20 nm for the silicon oxide layer, as estimated from *in situ* quartz crystal microbalance measurements. For PM-IRRAS measurements, wafers thus produced were cut into suitable pieces (Disco DAD-321 saw, Disco Corp., Tokyo, Japan), cleaned in an ultrasonic bath with 5% surfactant solution (Extran MA02 neutral, Merck, Darmstadt, Germany), copiously rinsed with ultrapure water, cleaned in an ultrasonic bath in ethanol and dried in an argon stream.

2.2. Wet chemistry

Selectively protein-resistant monolayers were made from biotin–NH–CH_2–CH_2(O–CH_2–CH_2)$_n$–NHCONH(CH_2)$_3$–Si(OEt)$_3$ (silane–PEG–biotin, (O–CH_2–CH_2)$_n$ section has M_w=2000 Da), which was obtained by custom synthesis from Rapp Polymere GmbH (Tübingen, Germany) and stored under argon. Proton nuclear magnetic resonance (^{1}H NMR) measurements suggested that the sample may be contaminated with biotin–NH–CH_2–CH_2(O–CH_2–CH_2)$_n$–NH–biotin, which is a likely byproduct of synthesis; as these molecules lack surface-anchoring triethoxysilane groups, they should be readily rinsed away and should not affect the properties of the eventual self-assembled monolayer. To form self-assembled monolayers, dry toluene (10 ml, 99.85%, extra dry, water <30 ppm, Acros Organics, Geel, Belgium) was added to a flask containing the substrate in a glove box under nitrogen (water <0.1 ppm), followed by silane–PEG–biotin (1–3 mg), before the flask was transferred to a Schlenk line where triethylamine (a few drops, previously distilled under an inert atmosphere) was added also under an inert atmosphere. The flask was sealed and heated briefly to between 80 and 150 °C, allowed to stand at room temperature for 24 h, and then incubated at 80 °C for 24 h, then rinsed successively with ethyl acetate, methanol and ethanol (all analytical grade) before being dried in a nitrogen stream and stored under nitrogen (water <0.1 ppm). Solutions for protein adsorption experiments were made using bovine serum albumin (Sigma Aldrich, St Louis, U.S.A.), streptavidin (from *Streptomyces avidinni*, lyophilized, Serva Electrophoresis, Heidelberg, Germany), and Dulbecco's phosphate buffered saline solution (pH 7.45, Gibco/Invitrogen, Carlsbad, U.S.A., solid tablets made up with ultrapure water (MilliQ Gradient A10 18.2 MΩ cm, Millipore, Billerica, USA). Glassware for these experiments was cleaned with surfactant (Hellmanex II, Hellma GmbH & Co. KG, Müllheim, Germany), rinsed with ultrapure water and then ethanol and dried in an argon stream.

2.3. Thin film characterization

2.3.1. Electron microscopy

A transmission electron microscopy (TEM) specimen was prepared using the conventional cross-section method. Unidirectional ion milling from the substrate to the film was performed using a low-angle ion milling and polishing system at 4 keV (Model 1010, E.A. Fischione Instruments Inc., Export, U.S.A.). Final polishing was performed at 0.5 keV. During the ion-milling process, the specimen was cooled with liquid nitrogen.

Conventional TEM was performed using a JEOL JEM 4000 FX (JEOL Ltd., Tokyo, Japan) operated at 400 kV.

Analytical TEM studies were carried out in a VG HB501UX dedicated scanning transmission electron microscope operated in ultra-high vacuum at an accelerating voltage of 100 kV. The beam current was 0.12 nA for a beam diameter of 0.7 nm (full width at half maximum (FWHM)). This microscope has a cold field emission source and is equipped with an energy-dispersive X-ray spectrometer (Noran System SIX, Thermo Fischer Scientific, Waltham, U.S.A.) and an electron energy-loss spectrometer (EELS) (Gatan UHV Enfina system, Gatan Inc., Pleasanton, U.S.A.). The energy resolution of the whole system was approximately 0.6 eV as determined by the FWHM of the zero-loss peak at a dispersion of 0.1 eV/channel.

2.3.2. X-ray photoelectron spectroscopy (XPS)

X-ray photoelectron spectroscopy was carried out using non-monochromated Mg Kα (1256.6 eV) X-rays from a Dual-Anode X-ray Source (Physical Electronics Inc., Chanhassen, U.S.A). Photoelectrons were detected using a hemispherical energy analyzer (Phoibos 150 from Specs GmbH, Berlin, Germany). All measurements were performed in normal emission geometry, at a vacuum of $\sim5\times10^{-10}$ mbar.

Peaks to be quantified were fitted, after subtraction of a Shirley background, with the following Gaussian–Lorentzian product formula:

$$\mathrm{GL}(x,F,E,m)=\frac{\exp\left(-4\ln 2(1-m)\frac{(x-E)^2}{F^2}\right)}{1+\frac{4m(x-E)^2}{F^2}} \quad (1)$$

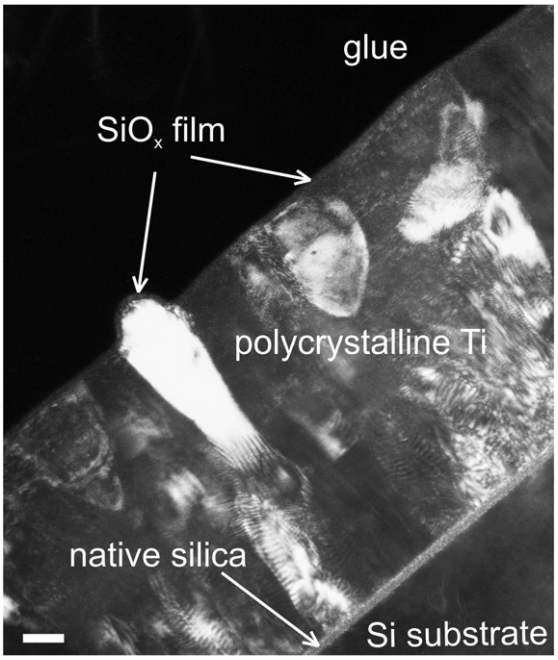

Fig. 1. Dark field TEM image of cross-sectional Si–Ti–SiO_x specimen. Scale bar represents 20 nm.

where x is the binding energy, E is the peak position in binding energy, F the peak width and m, which controls the relative weight of Gaussian and Lorentzian character, was fixed at 0.1 throughout.

2.3.3. X-ray reflectivity

The X-ray reflectivity measurements were performed using a two-circle X-ray reflectometer (XRD 3003 TT, Seifert Analytical X-ray, Ahrensburg, Germany) with a copper anode and an NaI scintillation counter. A Ni/C multilayer mirror and a germanium channel-cut crystal give a monochromatic and parallel beam with $\lambda = 1.54$ Å (Cu $K_{\alpha 1}$). The chosen slits resulted in an angular resolution of ~0.01°. A dynamic range of more than seven orders of magnitude can be covered with automatic beam attenuators.

2.4. Simulations

Simulations of the PM-IRRAS signal from different substrates were made using Hansen's notation of the Fresnel matrix formalism, implemented in Igor Pro (Wavemetrics Inc., Lake Oswaego, U.S.A.) [21]. Using this method, the polarization-dependent reflectivity of multilayer systems and the signal from different layers could be determined. Tabulated values were used for the optical constants of silicon oxide [22] and titanium [23].

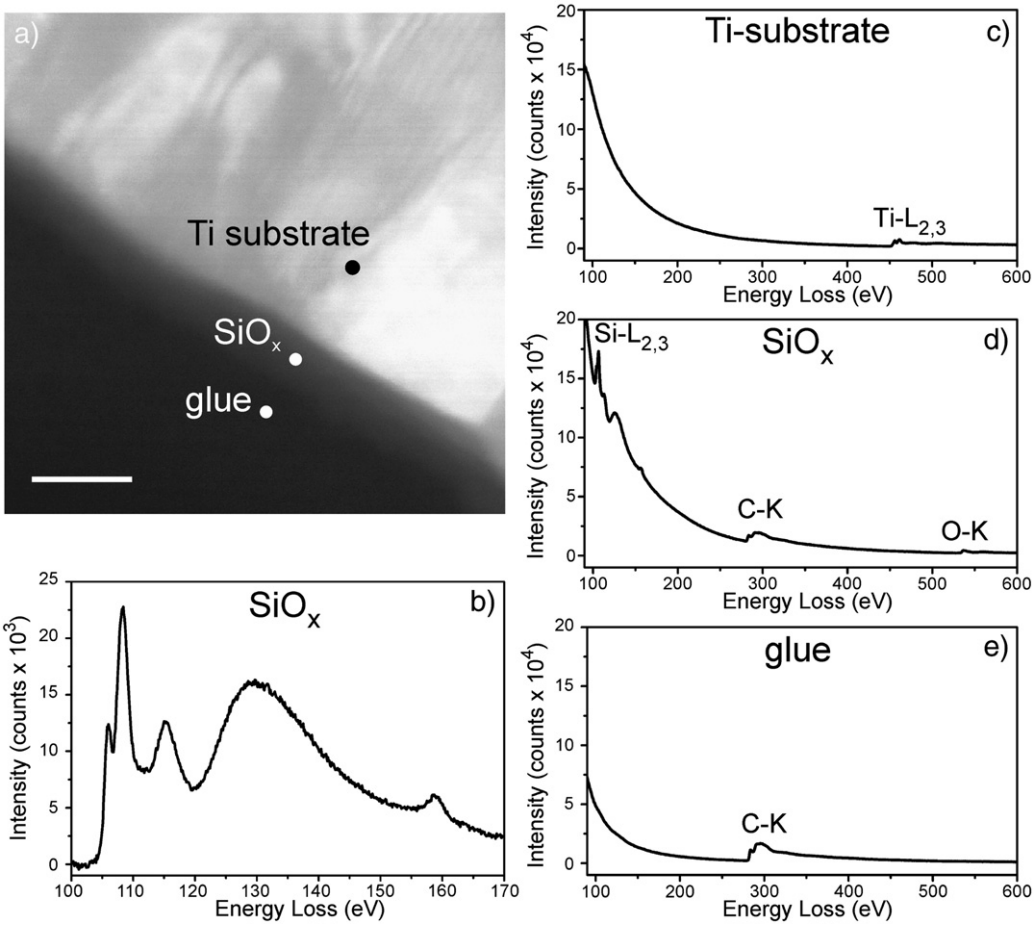

Fig. 2. HAADF-STEM and EELS characterization of Si–Ti–SiO_x substrate. a) HAADF-STEM image of a cross-sectional TEM specimen. Scale bar represents 20 nm. c) d) e) EELS spectra recorded in the energy range of Si–$L_{2,3}$, C–K, Ti–$L_{2,3}$ and O–K edges from the regions indicated in image (a). b) Background-subtracted Si–$L_{2,3}$ edge acquired at a position similar to that of (d).

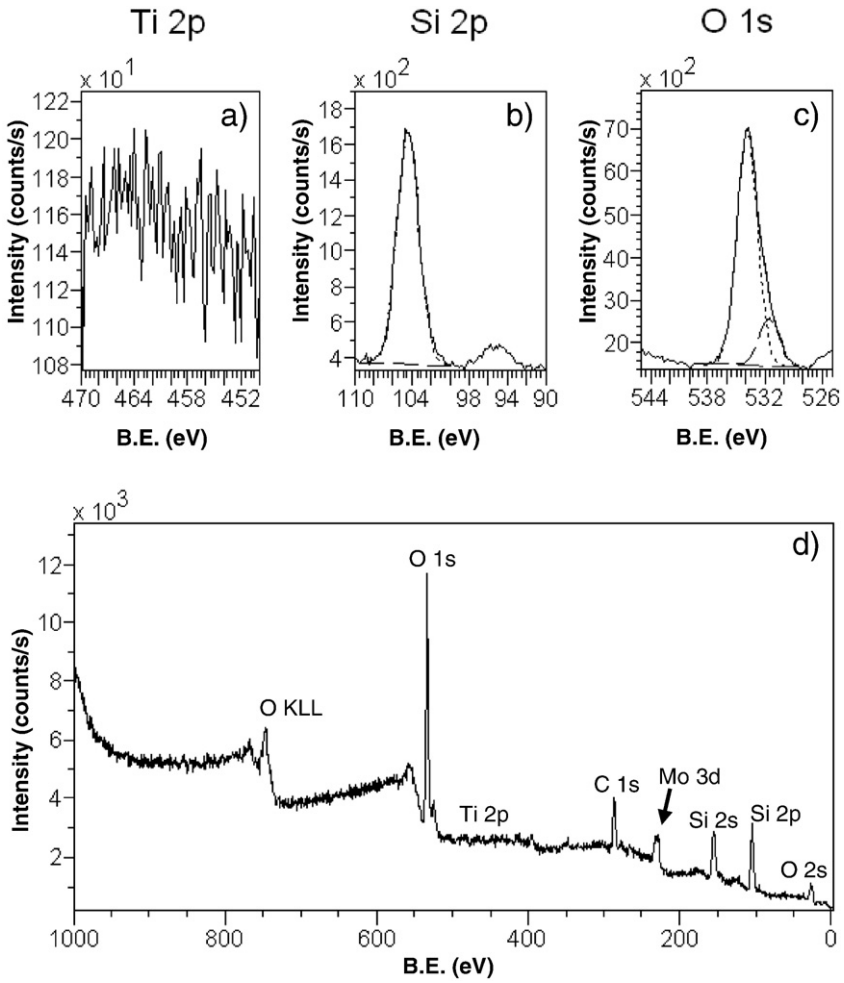

Fig. 3. XPS spectrum of the Si–Ti–SiO_x substrate. Graphs show intensity in counts per second versus binding energy (B.E.) in eV. Detailed scans of the a) Ti 2p, b) Si 2p and c) O 1s regions: solid lines show measured spectra, near-horizontal dashed lines show fitted Shirley backgrounds and other dashed lines show fits to the measured spectra using Gaussian–Lorentzian functions as described in the text. The small peaks approximately 10 eV to the right of the main peaks in the Si 2p and O 1s regions can be ignored as they are almost certainly due to the presence of Mg $K\alpha_3$ radiation in the exciting X-rays. d) Overview of the entire spectrum. The C 1s peak may arise from contamination and/or adsorbed CO_2, as may the subsidiary O 1s peak at 531.6 eV. The Mo 3d peak is due to the sample holder.

2.5. Polarization-modulated infrared spectroscopy (PM-IRRAS)

PM-IRRAS measurements were performed on a Bruker Vertex 70 infrared spectrometer with a PMA 50 unit (Bruker Optik GmbH, Ettlingen, Germany). The half-wave retardation was set to 1500 cm^{-1}. Spectra were measured with a resolution of 4 cm^{-1}, the angle of incidence was 70° and 256 scans were co-added. Before each measurement, the spectrometer and the sample chamber were rinsed with dry, carbon dioxide-free air for 300 s. The PM-IRRAS setup has been described [7]. The polarization of the incident beam is changed periodically between s- and p-polarization by the polarization modulation (PM) unit; this leads to a fast modulation of the signal. The difference between the s- and p-polarized signals is measured using a lock-in amplifier, and is normalized using the average signal, measured using a low-pass filter. The IR-signal is convolved with a double cosine function due to the polarization modulation. This function can be expanded in a sum of Bessel functions: usually only the zeroth and second order Bessel functions contribute to the reflectivity signal (Eq. (2)) and have to be corrected for during data processing. This is done as described elsewhere [7]. The resulting measured reflectivity, R, is given by [24,25]

$$R = C\frac{J_2(\varphi_0)(R_p - R_s)}{(R_p + R_s) + J_0(\varphi_0)(R_p - R_s)} \quad (2)$$

where R_p and R_s are the reflectivities of the surface to s- and p-polarized light, φ_0 is the amplitude of the oscillating phase shift introduced by the PM, C is an instrumental constant, and J_n signifies a Bessel function of order n.

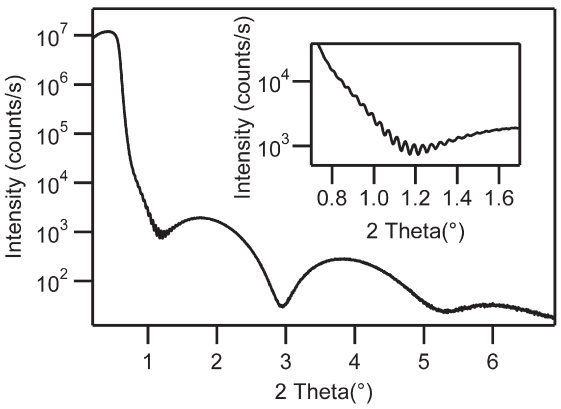

Fig. 4. X-ray reflectivity of the Si–Ti–SiO_x substrate, measured using Cu K_α radiation. The interference fringes demonstrate the formation of well-defined interfaces and reveal the thicknesses of the SiO_x and Ti layers. The narrow fringes (enlarged in the inset) correspond to a Ti thickness of 212 nm, whereas the broad fringes yield an SiO_x thickness of 6.4 nm.

3. Results and discussion

3.1. Characterization of Si–Ti–SiO_x substrates

The structure of the novel Si–Ti–SiO_x substrates is illustrated by a dark field (DF) transmission electron microscopy (TEM) image of the cross section in Fig. 1. The titanium film lies on top of the silicon wafer and its native oxide layer. In this DF image, the polycrystalline nature of the titanium film is clearly visible. The silicon oxide film on top of the titanium film is visible, and appears to be of roughly uniform thickness (of the order of 5 nm) and to smoothly follow the titanium surface. Since the titanium film is polycrystalline, its surface is not entirely flat, but is rather punctuated by crystallites that rise out of the surface, as in the centre of Fig. 1. (Images of other areas suggest that these features may be more common than shown in Fig. 1.)

A high-angle annular dark field (HAADF) scanning transmission electron microscopy (STEM) image of the surface is shown in Fig. 2a. Electron energy-loss spectroscopy (EELS) measurements were performed in the various regions, i.e. the titanium substrate, the silicon oxide film and the glue used for the TEM sample preparation. The different spectra for the titanium substrate, the silicon oxide film and for the glue are shown in the energy region between 90 and 600 eV in Fig. 2c,d,e, and confirm the chemical identity of the deposited films. The Si–$L_{2,3}$ electron energy-loss near-edge structure of the SiO_x film corrected for the background is shown in Fig. 2b. This spectrum contains two initial sharp peaks that are followed by a sharp and a broad peak and have been attributed to electron excitation into molecular orbitals associated with a silicon atom that is tetrahedrally coordinated [26,27].

Our intention was to investigate a silicon oxide, and not a titanium or titanium oxide surface; it is thus essential that the titanium layer should be completely or almost completely covered by the silicon oxide layer over the whole of the substrate. This is shown to be the case by the X-ray photoelectron spectrum (XPS) of the surface (Fig. 3), which shows peaks in the Si 2p and 2s and O 1s and 2s regions, but no discernable peak in the Ti 2p region. The sampled area was of the order of square millimeters. The relative values of the areas under the Si 2p and O 1s peaks (Fig. 3b, c), combined with tabulated sensitivity factors [28], give an atomic silicon to oxygen ratio of $1.5^{+0.3}_{-0.0}$. The fact that no titanium peak can be observed suggests that the silicon oxide film thickness is at least a few times the electron attenuation length in silicon oxide, which has been measured to be of the order of 2–3 nm [29], but may vary strongly with film density and microstructure; this is consistent with the film thickness observed by TEM.

To measure the exact thickness of the Ti and SiO_x films on the Si substrate we performed X-ray reflectivity measurements (see Fig. 4). The data show distinct Kiessig oscillations which arise from the interference of X-rays reflected from the different interfaces and can be used to calculate the thickness d according to $d=2\pi/\Delta q$, where

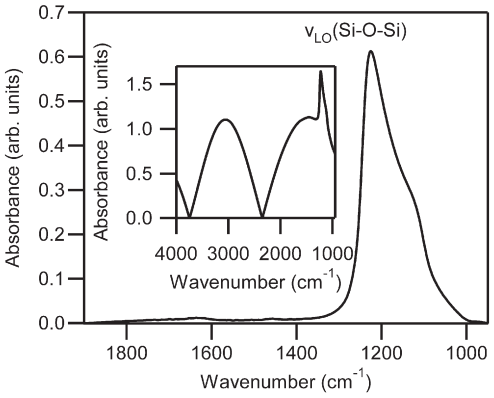

Fig. 6. PM-IRRAS spectrum of non-functionalized Si–Ti–SiO_x substrate. Inset shows spectrum before, and main figure after removal of the Bessel function envelope.

Δq is the periodicity of the oscillations in reciprocal space ($q=4\pi\lambda^{-1}\sin\theta$, where λ is the wavelength and θ the incidence angle).

The narrow fringes shown in the inset to Fig. 4 originate from the 212 nm thick Ti layer, whereas the broad fringes correspond to the 6.4 nm thick SiO_x layer on top. Both thicknesses confirm the (local) values found by TEM measurements on a macroscopic length scale. Moreover, the data shown in Fig. 4 indicate well-defined interfaces with moderate roughness for this particular sample. Because other samples showed increased roughness, we did not analyze the data in more detail.

3.2. Simulations of PM-IRRAS on Si–Ti–SiO_x substrates

To enable optimization of the signal and to determine the influence of the thickness of the silicon oxide layer on the signal strength, simulations of the PM-IRRAS signal were performed as described in 'Materials and methods'. We used a model consisting of a semi-infinite titanium layer, a silicon oxide layer whose thickness was varied between 5 nm and 50 nm, and an organic layer with a thickness of 15 nm, which generated the specific infrared absorption signal. For simplicity, smooth interfaces were assumed.

As shown in Fig. 5, the simulated signal from the organic layer is strongly angle-dependent, with an optimum (highest signal to noise ratio) angle of incidence around 74° from the surface normal. Importantly, the simulated signal is only slightly attenuated by the presence of the silicon oxide film, especially at the lowest film thicknesses. For a 5 nm thick silicon oxide film, which corresponds approximately to the Si–Ti–SiO_2 substrates used in this study, the signal is almost the same as that from an organic film on bare titanium, confirming that these substrates should indeed enable PM-IRRAS measurements of a similar quality to those performed on a metal surface.

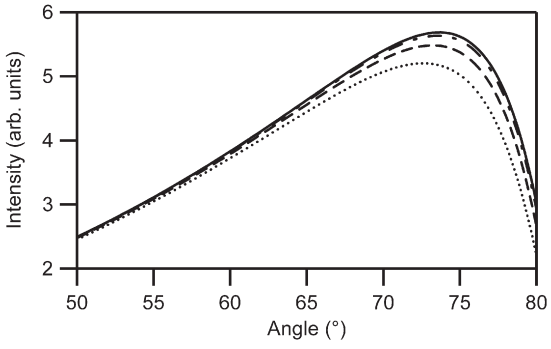

Fig. 5. Simulation of the PM-IRRAS signal from an organic thin film (15 nm thick) which is separated from a semi-infinite titanium substrate by a silicon oxide film of thickness: no silicon oxide (——), 5 nm (– · – · –), 20 nm (– – – –), 50 nm (·····).

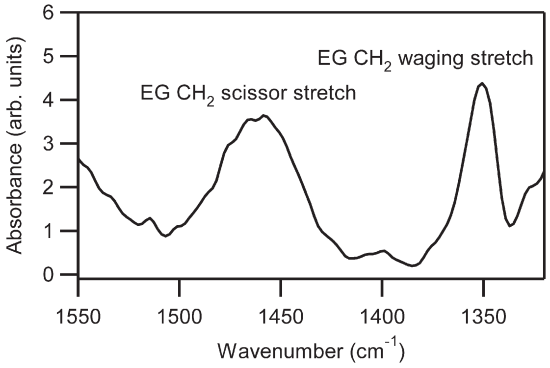

Fig. 7. Background-subtracted PM-IRRAS spectrum of Si–Ti–SiO_x that has been functionalized with silane–PEG–biotin.

3.3. PM-IRRAS measurements on Si–Ti–SiO_x substrates

A typical PM-IRRAS spectrum of a clean, non-functionalized Si–Ti–SiO_x substrate surface is shown in the inset to Fig 6. There are strong absorption bands from the silicon oxide film in the range 1000 to 1250 cm^{-1}; this region of the spectrum after removal of the Bessel function envelope is shown in the main part of Fig. 6. Bands at 1225 cm^{-1} and 1178 cm^{-1} (broader band, visible as a shoulder) can be distinguished, and both may be attributed to longitudinal optical (LO) ν_{LO} (Si–O–Si) stretching modes. The two bands are associated with differing Si–O bond angles and thus with the details of the local coordination of silicon atoms by oxygen atoms. The relative strength of these two bands is known to depend in general on the overall silicon to oxygen ratio — the band at 1178 cm^{-1} has been associated with SiO, with the band at 1225 cm^{-1} being associated with SiO_2 — as well as on the details of the local film structure [30].

As a proof of principle for the practical use of the Si–Ti–SiO_x substrate in PM-IRRAS, we now describe a series of measurements designed to investigate the protein adsorption properties of a selectively protein-resistant self-assembled monolayer of biotin–NH–CH_2–CH_2(O–CH_2–CH_2)$_n$–NHCONH(CH_2)$_3$–Si(OEt)$_3$ (silane–PEG–biotin), which was designed to enable the production of a surface that strongly binds streptavidin, although remaining resistant to other protein molecules. The resistance to protein adsorption of surfaces functionalized with poly(ethylene glycol) is well known, and silane-functionalized poly(ethylene glycol) molecules have previously been used to render silicon oxide surfaces protein resistant [31–34]; our silane–PEG–biotin molecule is similar to the silane–PEG–methoxy of Blümmel et al. [31]. The binding of biotin to the protein streptavidin is one of the strongest non-covalent interactions known, with an association equilibrium constant of order 10^{13} M^{-1}, and is also highly specific [35]. Since each streptavidin molecule has four biotin binding sites, streptavidin could be used as a linker for example to bind a chosen biotinylated protein molecule to the substrate surface. Silane-anchored, biotin-terminated PEG has been previously used to produce a surface that repels most proteins but can be functionalized with streptavidin [36–40]; to the best of our knowledge, the present study is the first time that this has been carried out using a one-step process involving the formation of a covalent bond to a silicon oxide substrate.

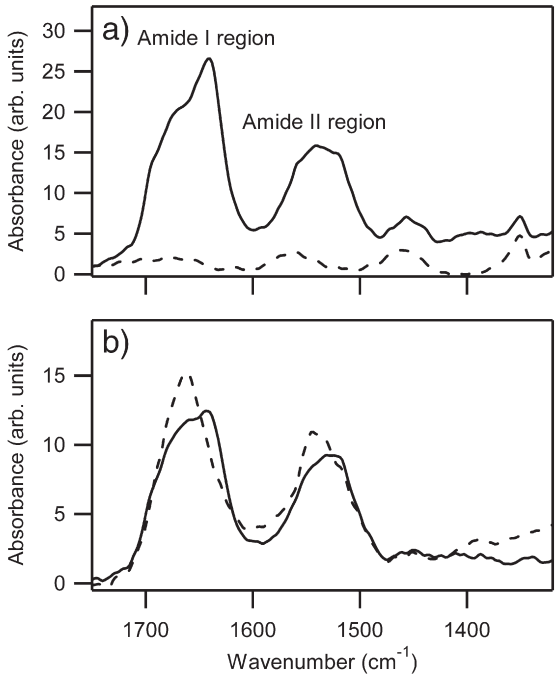

Fig. 8. Selective adsorption of protein molecules by silane–PEG–biotin-functionalized silicon oxide surface. PM-IRRAS spectra measured on Si–Ti–SiO_x substrate surfaces that have been incubated in protein solutions, rinsed and dried. a) Silane–PEG–biotin functionalized surfaces following incubation in solutions of streptavidin (0.1 mg/ml in PBS, solid line) and BSA (1.0 mg/ml in PBS, dashed line). b) Control experiments on bare surfaces following incubation in solutions of streptavidin (0.1 mg/ml in PBS, surface heated with toluene and triethylamine as control for PEG–biotin reaction, solid line) and BSA (1.0 mg/ml in PBS, surface heated with toluene and triethylamine, dashed line). Incubation time 50 min (all spectra). Spectra of bare substrates have been subtracted.

A typical PM-IRRAS spectrum of an Si–Ti–SiO_x substrate surface that has been functionalized with silane–PEG–biotin is shown in Fig. 7. Because of the interference with the silicon oxide absorption bands, the strong C–O–C stretching mode could not be monitored. Nevertheless, other significant vibrational modes of PEG are visible: the ethylene glycol wagging mode (1350 cm^{-1}) and the ethylene glycol scissoring mode (1463 cm^{-1}) [41].

Fig. 8 shows the PM-IRRAS spectra of blank and silane–PEG–biotin-functionalized Si–Ti–SiO_x substrates that have been exposed to aqueous solutions of bovine serum albumin (BSA) and streptavidin respectively. It can be seen from the presence of strong amide I (1664 cm^{-1}) and amide II (1540 cm^{-1}) peaks that BSA has adsorbed in significant quantities to the blank substrate, as expected for a silicon oxide surface [42]. In contrast, there is no discernable BSA on the silane–PEG–biotin-coated surface. When similar surfaces are exposed to aqueous streptavidin solutions, however, significant amounts of streptavidin are seen to adsorb to the silane–PEG–biotin surface. These results thus demonstrate that the silane–PEG–biotin-functionalized surface has its intended properties of binding streptavidin, but resisting the adsorption of other proteins.

4. Conclusion

We have demonstrated that successively sputtered thin films of titanium and silicon oxide provide a valuable substrate for PM-IRRAS measurements of self-assembled monolayers on silicon oxide surfaces, and have used such measurements to characterize the protein adsorption properties of a silane-anchored selectively protein-resistant self-assembled monolayer.

Acknowledgements

We acknowledge expert technical assistance from Reinhart Völker (thin film deposition) and Michael Pudleiner (XPS). We acknowledge Roberto Fiammengo (^{1}H NMR). IED acknowledges a Humboldt Research Fellowship from the Alexander von Humboldt Foundation. FS gratefully acknowledges support by EPSRC and Landesstiftung Baden-Württemberg foundation. This publication and the project described were also partly supported by the National Institutes of Health through the NIH Roadmap for Medical Research (PN2 EY016586) and by the Max Planck Society.

References

[1] T. Buffeteau, B. Desbat, J.M. Turlet, Appl. Spectrosc. 45 (1991) 380.
[2] V. Zamlynny, J. Lipkowski, in: R.C. Alkire, D.M. Kolb, J. Lipkowski, P.N. Ross (Eds.), Diffraction and Spectroscopic Methods in Electrochemistry, vol. 9, Wiley-VCH Verlag, Weinheim, Germany, 2006, p. 315.
[3] V. Zamlynny, I. Zawisza, J. Lipkowski, Langmuir 19 (2003) 132.
[4] R.G. Greenler, J. Chem. Phys. 44 (1966) 310.
[5] D. Käfer, G. Witte, P. Cyganik, A. Terfort, C. Woll, J. Am. Chem. Soc. 128 (2006) 1723.
[6] H. Hoffmann, U. Mayer, A. Krischanitz, Langmuir 11 (1995) 1304.
[7] M.W.A. Skoda, R.M.J. Jacobs, J. Willis, F. Schreiber, Langmuir 23 (2007) 970.
[8] I. Zawisza, G. Wittstock, R. Boukherroub, S. Szunerits, Langmuir 23 (2007) 9303.
[9] A.E. Dowrey, C. Marcott, Appl. Spectrosc. 36 (1982) 414.
[10] J.C. Riviere, Surface Analytical Techniques, Clarendon Press, Oxford, 1990.
[11] E.A. Cavalcanti-Adam, T. Volberg, A. Micoulet, H. Kessler, B. Geiger, J.P. Spatz, Biophys. J. 92 (2007) 2964.
[12] R. Ivkov, P.D. Butler, S.K. Satija, L.J. Fetters, Langmuir 17 (2001) 2999.
[13] D.C. McDermott, D. Kanelleas, R.K. Thomas, A.R. Rennie, S.K. Satija, C.F. Majkrzak, Langmuir 9 (1993) 2404.
[14] D.K. Kambhampati, T.A.M. Jakob, J.W. Robertson, M. Cai, J.E. Pemberton, W. Knoll, Langmuir 17 (2001) 1169.
[15] S. Bharathi, M. Nogami, S. Ikeda, Langmuir 17 (2001) 1.

[16] S. Szunerits, Y. Coffinier, S. Janel, R. Boukherroub, Langmuir 22 (2006) 10716.
[17] K. Glasmastar, C. Larsson, F. Hook, B. Kasemo, J. Colloid Interface Sci. 246 (2002) 40.
[18] F. Schreiber, Prog. Surf. Sci. 65 (2000) 151.
[19] F. Schreiber, J. Phys., Condens. Matter 16 (2004) R881.
[20] D.K. Schwartz, Annu. Rev. Phys. Chem. 52 (2001) 107.
[21] M.W.A. Skoda, D.Phil. Thesis, Oxford University, Oxford, 2007.
[22] E.D. Palik (Ed.), Handbook of Optical Constants of Solids, Academic Press, Inc., New York, U.S.A., 1985.
[23] D.W. Lynch, C.G. Olson, J.H. Weaver, Phys. Rev. B 11 (1975) 3617.
[24] R. Mendelsohn, J.W. Brauner, A. Gericke, Annu. Rev. Phys. Chem. 46 (1995) 305.
[25] K.W. Hipps, G.A. Crosby, J. Phys. Chem. 83 (1979) 555.
[26] L.A.J. Garvie, A.J. Craven, R. Brydson, Am. Mineral. 79 (1994) 411.
[27] L.A.J. Garvie, P.R. Buseck, Am. Mineral. 84 (1999) 946.
[28] J.F. Moulder, W.F. Stickle, P.E. Sobol, K.D. Bomben, Handbook of X-ray Photoelectron Spectroscopy, Perkin Elmer Corp., Physical Electronics Division, Eden Prarie, M.N., U.S.A., 1992.
[29] H. Ebel, M.F. Ebel, R. Svagera, A. Hofmann, Surf. Interface Anal. 18 (1992) 821.
[30] V.P. Tolstoy, I. Chernyshova, V.A. Skryshevsky, Handbook of Infrared Spectroscopy of Ultrathin Films, John Wiley & Sons, Hoboken, U.S.A., 2002.
[31] J. Bluemmel, N. Perschmann, D. Aydin, J. Drinjakovic, T. Surrey, M. Lopez-Garcia, H. Kessler, J.P. Spatz, Biomaterials 28 (2007) 4739.
[32] A.A. Brown, N.S. Khan, L. Steinbock, W.T.S. Huck, Eur. Polym. J. 41 (2005) 1757.
[33] S. Sharma, T.A. Desai, J. Nanosci. Nanotechnol. 5 (2005) 235.
[34] A. Papra, A. Bernard, D. Juncker, N.B. Larsen, B. Michel, E. Delamarche, Langmuir 17 (2001) 4090.
[35] D.E. Hyre, I. Le Trong, E.A. Merritt, J.F. Eccleston, N.M. Green, R.E. Stenkamp, P.S. Stayton, Protein Sci. 15 (2006) 459.
[36] S.W. Metzger, M. Natesan, C. Yanavich, J. Schneider, G.U. Lee, J. Vac. Sci. Technol., A 17 (1999) 2623.
[37] N.P. Huang, J. Voros, S.M. De Paul, M. Textor, N.D. Spencer, Langmuir 18 (2002) 220.
[38] R.C. Gunawan, J.A. King, B.P. Lee, P.B. Messersmith, W.M. Miller, Langmuir 23 (2007) 10635.
[39] Y.H. Jang, S.Y. Oh, J.K. Park, Enzyme Microb. Technol. 39 (2006) 1122.
[40] E.V. Amirgoulova, J. Groll, C.D. Heyes, T. Ameringer, C. Rocker, M. Moller, G.U. Nienhaus, ChemPhysChem 5 (2004) 552.
[41] T. Miyazawa, Y. Ideguchi, K. Fukushima, J. Chem. Phys. 37 (1962) 2764.
[42] S.J. McClellan, E.I. Franses, Colloids Surf., A 260 (2005) 265.